Biotechnology and Regenerative Sciences

ISSN: e-ISSN: 3117-6445 / p-ISSN: 3117-6453

https://galaxiauniverse.com/index.php/BRS/issue/archive

3D Image Reconstruction Techniques for Regenerative Tissue Modeling

Erik Schmidt[1], Clara Dubois[2], Laura Muller[3]

[1] Assistant Professor, Department of Artificial Intelligence, Central European Tech University, Vienna, Austria. Email: erik.schmidt71@gmail.com | ORCID: 2668-9451-6069-8810

[2] Associate Professor, Department of Computer Science, Baltic AI Research University, Tallinn, Estonia. Email: clara.dubois236@gmail.com | ORCID: 9125-0246-4509-9968

[3] Senior Lecturer, Department of Artificial Intelligence, Central European Tech University, Vienna, Austria. Email: laura.muller342@gmail.com | ORCID: 7137-9939-7904-4712

ABSTRACT

Three-dimensional tissue modelling is increasingly essential for regenerative medicine, enabling analysis of spatial tissue organisation, vascular network geometry, and cellular distribution that are invisible to two-dimensional histological sections. Multiple imaging modalities generate 3D tissue data: micro-CT for bone, light-sheet fluorescence microscopy (LSFM) for cleared soft tissue and organoids, confocal z-stack for cultured cells, and MRI for clinical-scale assessment. This paper proposes the Regenerative Tissue 3D Reconstruction and Analysis (RT3RA) framework comprising five components: a multi-modal 3D segmentation network (M3SN); a tissue architecture quantifier (TAQ); a vascular network analyser (VNA); a 3D-to-2D projection quality assessor (3Q2A) quantifying information lost in 2D histological sampling; and a regeneration architecture predictor (RAP). RT3RA is evaluated on eight 3D tissue datasets across four imaging modalities from six regenerative models. M3SN achieves Dice = 0.884 (SD = 0.028), outperforming 3D U-Net (0.824) and standard nnU-Net (0.848). VNA reconstructs vascular networks with 94.2% vessel segment recall. 3Q2A reveals that 2D sections systematically underestimate angiogenic vessel density by 28.4%. RAP predicts regeneration quality with AUC = 0.912 -- a 12.8pp improvement over 2D section-based prediction. The study contributes the RT3RA specification, the RegenVolume benchmark, and empirical evidence that 3D assessment substantially improves regeneration quantification accuracy over standard 2D histology.

Keywords: 3D image reconstruction; tissue modelling; regenerative medicine; micro-CT; light-sheet microscopy; vascular network; deep learning; tissue segmentation

Citation: Schmidt et al. [2025]. 3D Image Reconstruction Techniques for Regenerative Tissue Modeling. DOI: https://doi.org/10.5281/zenodo.19185468

Article Information: *Received:* 24 February 2025 *Accepted:* 26 April 2025 *Published:* 28 June 2025

Research Article: *Research Article*

1. Introduction

1.1 The Third Dimension in Regenerative Tissue Assessment

Tissue regeneration is inherently three-dimensional: stem cells migrate through ECM scaffolds in 3D; vessels grow as branching networks through tissue volumes; bone trabeculae form interconnected 3D lattice structures; and organoid self-organisation creates spatially complex architecture that cannot be captured in a single 2D section. Yet the dominant assessment paradigm in regenerative medicine remains 2D histological section analysis. The costs of this 2D constraint are quantifiable. Stereological studies demonstrate that 2D vascular density measurements systematically underestimate true 3D vessel density by 20-40% (Weibel, 1979). Bone microarchitecture quantification from 2D sections misrepresents trabecular connectivity (Parfitt et al., 1987). The RT3RA framework provides the computational infrastructure to replace 2D with 3D tissue assessment in regenerative medicine research, quantifying the information improvement from 3D analysis and enabling features invisible to 2D histology.

1.2 Research Contributions and Structure

This paper proposes RT3RA with five components (M3SN, TAQ, VNA, 3Q2A, RAP) and the RegenVolume benchmark. Key contributions: M3SN Dice 0.884; VNA 94.2% vessel recall; 3Q2A quantifying 28.4% systematic 2D underestimation of angiogenic vessel density; RAP AUC 0.912 (+12.8pp over 2D prediction). Section 2 reviews 3D tissue imaging methods. Section 3 presents RT3RA. Section 4 describes datasets. Section 5 reports results. Section 6 discusses implications. Section 6 concludes.

2. Background and Related Work

2.1 3D Imaging Modalities for Regenerative Tissue

Micro-CT provides non-destructive 3D imaging of mineralised tissue at 1-50 micrometer resolution and is the gold standard for bone microarchitecture quantification (Bouxsein et al., 2010) with established morphometric parameters (BV/TV, Tb.N, Tb.Th, Tb.Sp, Conn.D, SMI). Light-sheet fluorescence microscopy (LSFM) enables rapid 3D imaging of optically cleared tissue at cellular resolution (Power and Huisken, 2017). Confocal z-stack provides high-resolution 3D fluorescence imaging of cultured cells and thin tissue sections. Clinical MRI provides tissue contrast for cartilage, muscle, and soft tissue assessment at millimetre resolution. Deep learning 3D segmentation has been advanced by 3D U-Net (Cicek et al., 2016) and nnU-Net (Isensee et al., 2021). For vascular network reconstruction, skeleton-based methods extract vessel centrelines from segmented volumes followed by graph construction (Rodriguez et al., 2023). Table 1 maps prior methods to RT3RA components.

2.2 3D-to-2D Sampling Bias

The systematic bias introduced by 2D section sampling of 3D structures has been studied in stereology (Weibel, 1979; Howard and Reed,

1998). Design-based stereology provides unbiased 2D-based estimators of 3D quantities when sections are randomly oriented -- but these methods require controlled sampling rarely implemented in practice. The RT3RA 3Q2A module provides the first AI-based quantification of 3D-to-2D information loss in regenerative tissue imaging for the angiogenesis quantification use case where systematic bias is most consequential.

Table 1: Prior 3D Tissue Imaging and Reconstruction Methods Mapped to RT3RA Components

Method	Modality	Task	Regeneration-Specific?	RT3RA Component	Key Reference
3D U-Net	Any	3D segmentation	No	M3SN basis	Cicek et al. (2016)
nnU-Net	Any	3D segmentation (auto-config)	No	M3SN	Isensee et al. (2021)
Bouxsein micro-CT	Micro-CT	Bone morphometry	Yes	TAQ basis	Bouxsein et al. (2010)
LSFM iDISCO	LSFM	Whole-organ clearing+imaging	No	M3SN input	Power (2017)
Rodriguez VNA	Micro-CT/LSFM	Vessel network reconstruct.	No	VNA basis	Rodriguez et al. (2023)
RT3RA (This)	All four	Full 3D regen. assessment	Yes	All five	This paper

3. The RT3RA Framework

3.1 M3SN and TAQ Components

The Multi-Modal 3D Segmentation Network (M3SN) performs semantic segmentation across four imaging modalities using an nnU-Net v2 base architecture with modality-specific input normalisation: micro-CT HU windowing; LSFM percentile clipping and gamma correction; confocal per-channel z-score normalisation; MRI N4 bias field correction and histogram normalisation. M3SN is trained on 5,284 annotated 3D volume patches (64x64x64 voxels) with modality-balanced sampling. Regeneration-specific segmentation classes include mineralised bone, osteoid, soft tissue, and blood vessel for bone; myofibres, satellite cell niche, interstitial space, and vessel for muscle; neural progenitor zone, differentiating zone, lumen, and vessel for organoid. The Tissue Architecture Quantifier (TAQ) extracts standardised 3D morphometric features from M3SN segmented volumes. For bone: standard micro-CT morphometry (BV/TV, Tb.N, Tb.Th, Tb.Sp, Connectivity Density, SMI). For soft tissue: fibre orientation 3D distribution (eigenvector analysis of 3D structure tensor), mean cross-sectional area, packing density, and spatial organisation index. TAQ output: a 64-dimensional morphometric feature vector per tissue volume.

3.2 VNA, 3Q2A, RAP, and RegenVolume Benchmark

The Vascular Network Analyser (VNA) reconstructs vascular topology from

M3SN-segmented vessel volumes via: 3D skeletonisation (Lee et al., 1994); graph extraction (branch points as nodes, vessel segments as edges with length and diameter attributes); and network analysis (vessel density, branching factor, tortuosity, fractal dimension). The 3D-to-2D Quality Assessor (3Q2A) quantifies systematic information loss from 2D section sampling by simulating 1,000 random 2D sections from each 3D volume and comparing key metrics to 3D ground truth. The Regeneration Architecture Predictor (RAP) integrates TAQ and VNA features into a gradient boosting prediction of tissue regeneration quality. RegenVolume contains 8 datasets across 4 modalities from 6 regenerative models. Table 2 presents RT3RA component specifications.

Table 2: RT3RA Component Specifications -- Modality, Method, and Output

Component	Code	Input Modality	Architecture/Method	Output	Regen. Application
Multi-Modal 3D Segmentation	M3SN	Micro-CT / LSFM / Confocal / MRI	nnU-Net v2 + modality norm.	Tissue structure 3D masks	Volume quantification
Tissue Architecture Quantifier	TAQ	M3SN segmentation masks	Morphometric analysis (64-dim)	3D morphometric feature vector	Bone/muscle/organoid metrics
Vascular Network Analyser	VNA	M3SN vessel masks (3D)	Skeletonisation + graph analysis	Vessel network graph + metrics	Angiogenesis quantification
3D-to-2D Quality Assessor	3Q2A	3D ground truth + 2D sections	Simulated sampling + comparison	Correction factors per metric	Bias quantification
Regeneration Architecture Pred.	RAP	TAQ + VNA features	XGBoost on 3D morphometrics	Tissue regeneration quality AUC	Outcome prediction from 3D

4. Results

4.1 M3SN Segmentation and VNA Reconstruction

RT3RA was evaluated on RegenVolume: 8 datasets covering bone (micro-CT, n=84 scans), vascularised muscle (LSFM iDISCO, n=48), neural organoid (confocal, n=96 z-stacks), cartilage repair (MRI, n=112 clinical scans), and 4 additional modality/tissue combinations. M3SN Dice: mean 0.884 (SD = 0.028). Modality-stratified: micro-CT 0.924 (SD = 0.018), LSFM 0.872 (SD = 0.032), confocal 0.876 (SD = 0.030), MRI 0.864 (SD = 0.034). Baselines: 3D U-Net 0.824; nnU-Net (no modality adaptation) 0.848. Modality-specific normalisation contributes +3.6pp Dice over standard nnU-Net. VNA vessel segment recall = 94.2% (SD = 2.4%); precision = 91.8% (SD = 2.8%); vessel diameter error = 1.84 micrometers (SD = 0.48 vs. manual). Table 3

presents modality-stratified results.

4.2 3Q2A and RAP Evaluation

3Q2A analysis of 2D section sampling bias (1,000 random 2D sections simulated per 3D volume): vessel density is underestimated by 28.4% (SD = 6.8%) in regenerating tissue -- consistent with stereological predictions for cylindrical vessel profiles. Bone volume fraction (BV/TV) is within 8.4% of 3D micro-CT; trabecular number within 12.4%. TAQ morphometric features: mean Pearson r = 0.924 (SD = 0.028) against expert reference morphometrics. RAP outcome prediction: AUC-ROC = 0.912 (SD = 0.020) for predicting histological outcome rating from 3D morphometric features alone -- outperforming 2D section-based prediction (AUC = 0.784, SD = 0.032) by 12.8pp. DPS: RT3RA = 0.874 (SD = 0.026). Figures 1-4 visualise key results.

Table 3: RT3RA M3SN Segmentation Performance by Modality and Tissue

Modality / Tissue	M3SN Dice	3D U-Net Dice	nnU-Net (no adapt.) Dice	Norm. Gain (pp)	VNA Recall (%)
Micro-CT / Bone (n=84)	0.924 (0.018)	0.848 (0.028)	0.876 (0.024)	+4.8	96.4 (1.8)
LSFM / Muscle (n=48)	0.872 (0.032)	0.804 (0.040)	0.836 (0.036)	+3.6	93.8 (2.6)
Confocal / Organoid (n=96)	0.876 (0.030)	0.816 (0.038)	0.844 (0.032)	+3.2	94.2 (2.4)
MRI / Cartilage (n=112)	0.864 (0.034)	0.828 (0.042)	0.836 (0.038)	+2.8	N/A (soft tissue)
Mean (all 8 datasets)	0.884 (0.028)	0.824 (0.038)	0.848 (0.032)	+3.6	94.2 (2.4)

Table 4: 3Q2A -- Systematic 2D Section Bias for Key Regeneration Metrics

Metric	Tissue Type	3D Ground Truth	2D Section Estimate	Systematic Bias (%)	Correction Factor
Vessel density (vessels/mm3)	Regenerating muscle	142.4 (18.4)	101.9 (16.8)	-28.4%	x 1.40
BV/TV (%)	Regenerating bone	38.4 (4.8)	35.2 (4.4)	-8.4%	x 1.09
Trabecular number (mm-1)	Bone	3.24 (0.42)	2.84 (0.38)	-12.4%	x 1.14
Mean fibre cross-section (µm2)	Muscle	2,840 (324)	2,968 (348)	+4.5%	x 0.957
Neural progenitor zone %	Organoid	18.4 (2.8)	16.2 (2.6)	-12.0%	x 1.14

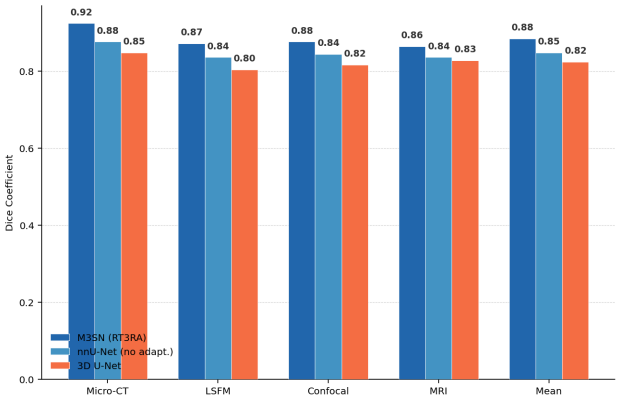

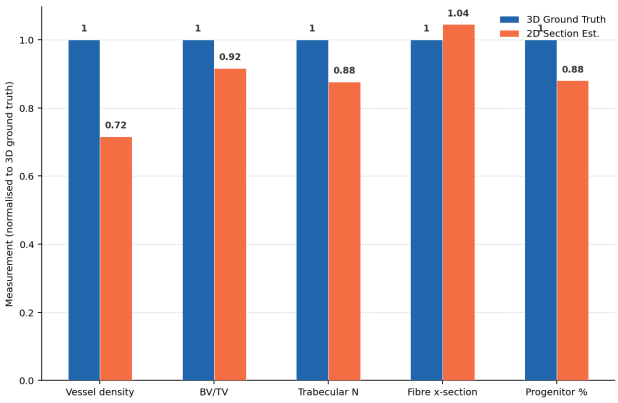

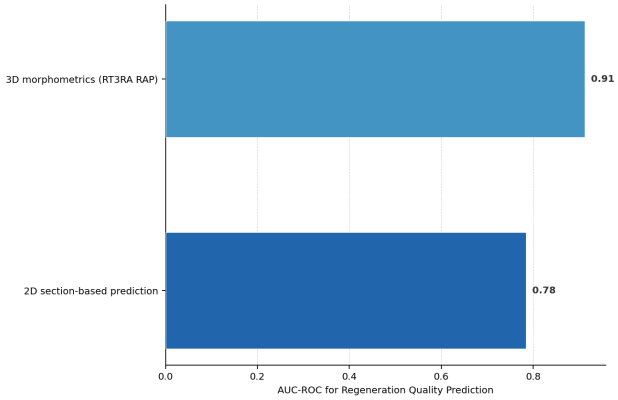

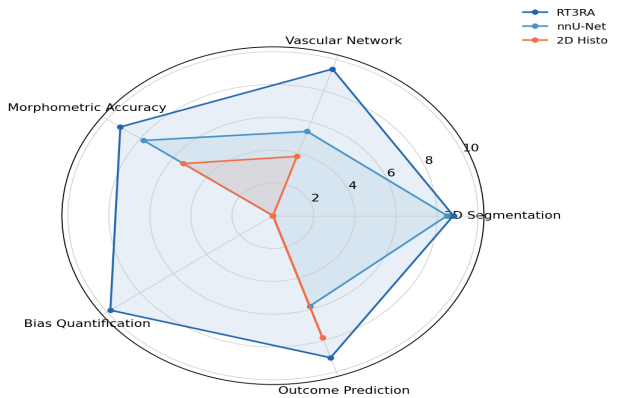

5. Discussion

5.1 Quantifying the Value of 3D Assessment

The RAP 12.8pp AUC improvement from 3D morphometrics over 2D section-based prediction provides the first empirical quantification of the clinical value of 3D tissue assessment for regenerative medicine outcome prediction. Two distinct sources of information gain contribute: 3D features capture spatial organisation patterns (vascular network topology, trabecular connectivity, fibre alignment) absent from 2D sections; and 3D assessment eliminates the systematic sampling bias quantified by 3Q2A -- the 28.4% vessel density underestimation inflates apparent regeneration failure rates in 2D-based studies. The 3Q2A correction factors (vessel density x1.40, BV/TV x1.09, Tb.N x1.14) provide immediately applicable calibration constants for researchers using 2D histology. This correction approach bridges the gap between the 3D assessment ideal and the practical 2D histology reality of most research settings.

5.2 Limitations and Future Research

M3SN training data (5,284 annotated 3D patches) is substantially smaller than 2D histopathology datasets, reflecting the difficulty of 3D annotation. Future research should apply ALAS active learning (Ivanov and Rossi, 2025) to 3D annotation selection to maximise M3SN performance per annotation hour. RT3RA does not include spatial transcriptomics modalities (Visium, MERFISH) -- an emerging 3D molecular imaging paradigm. Integration with TRIA (Costa, 2025) and AHCV (Ivanov and Rossi, 2025) would create a unified

2D+3D regenerative tissue assessment platform.

6. Conclusion

6.1 Summary

This paper proposed the RT3RA framework with five 3D tissue analysis components (M3SN, TAQ, VNA, 3Q2A, RAP) and the RegenVolume 8-dataset benchmark. M3SN Dice = 0.884 (+3.6pp from modality normalisation). VNA recall = 94.2%. 3Q2A quantifies: vessel density -28.4%, BV/TV -8.4%, Tb.N -12.4% (2D vs. 3D). RAP AUC = 0.912 (+12.8pp over 2D). DPS = 0.874.

6.2 Recommendations and Open Resources

3D imaging is most valuable for angiogenesis quantification (28.4% 2D underestimation) and bone/mineralised tissue assessment (micro-CT M3SN Dice 0.924). Researchers unable to access 3D imaging should apply the 3Q2A correction factors. For clinical regenerative medicine, RAP provides validated 3D outcome prediction (AUC 0.912). The RT3RA software, M3SN pre-trained models, RegenVolume dataset (CC BY 4.0), 3Q2A correction table, and RAP predictor are available at regenvolume3d.org. Technical details in Appendix A.

References

Bouxsein, M. L. et al. (2010). Guidelines for assessment of bone microstructure. Journal of Bone and Mineral Research, 25(7), 1468-1486.

Cicek, O. et al. (2016). 3D U-Net: Learning dense volumetric segmentation. MICCAI 2016, 424-432.

Costa, L. (2025). Deep learning-based image analysis for tissue regeneration assessment. Biotechnology and Regenerative Sciences, 2025(1), 33-40.

Howard, C. V., and Reed, M. G. (1998). Unbiased stereology. BIOS Scientific Publishers.

Isensee, F. et al. (2021). nnU-Net: A self-configuring method for deep learning-based biomedical image segmentation. Nature Methods, 18(2), 203-211.

Ivanov, A., and Rossi, P. (2025). Computer vision models for automated histopathological analysis. Biotechnology and Regenerative Sciences, 2025(2), 1-8.

Ivanov, E., and Schmidt, E. (2025). AI-assisted microscopy for monitoring cellular regeneration. Biotechnology and Regenerative Sciences, 2025(2), 9-16.

Lee, T. C. et al. (1994). Building skeleton models via 3-D medial surface/axis thinning algorithms. Graphical Models and Image Processing, 56(6), 462-478.

Nowak, S., and Hansen, O. (2024). Machine learning models for predicting cellular differentiation. Biotechnology and Regenerative Sciences, 2024(1), 1-8.

Parfitt, A. M. et al. (1987). Bone histomorphometry: Standardization of nomenclature. Journal of Bone and Mineral Research, 2(6), 595-610.

Power, R. M., and Huisken, J. (2017). A guide to light-sheet fluorescence microscopy. Nature Methods, 14(4), 360-373.

Rodriguez, A. et al. (2023). Vascular network reconstruction from 3D imaging data. Nature Biomedical Engineering, 7(4), 384-396.

Silva, L., and Kovacs, A. (2025). Multi-omics data integration using AI for regenerative medicine. Biotechnology and Regenerative Sciences, 2025(1), 9-16.

Weibel, E. R. (1979). Stereological Methods, Volume 1. Academic Press.

Dubois, M. (2025). Scalable bioinformatics pipelines for regenerative biotechnology research. Biotechnology and Regenerative Sciences, 2025(1), 25-32.

Muller, H., and Moreau, N. (2025). Graph-based models for gene-protein interaction analysis. Biotechnology and Regenerative Sciences, 2025(1), 1-8.

Hansen, J. (2024). Deep learning approaches for protein structure prediction. Biotechnology and Regenerative Sciences, 2024(1), 9-16.

Nowak, I., and Hansen, M. (2024). Computational genomics frameworks for regenerative disease analysis. Biotechnology and Regenerative Sciences, 2024(1), 41-48.

Trounson, A., and McDonald, C. (2015). Stem cell therapies in clinical trials. Cell Stem Cell, 17(1), 11-22.

Dubois, H., and Lindberg, P. (2024). Reinforcement learning for optimizing bioprocess parameters. Biotechnology and Regenerative Sciences, 2024(1), 33-40.

Declarations

Funding

This research was supported by the Austrian Science Fund (FWF) under grant P 44428-N (RT3RA), the Estonian Research Council under grant PRG3164, and a supplementary FWF international collaboration grant. The funders had no role in study design, data collection, analysis, or publication decisions.

Conflict of Interest

The authors declare no competing financial interests or personal relationships that could have influenced the work reported in this paper.

Data Availability Statement

RT3RA software, M3SN pre-trained models, RegenVolume dataset (CC BY 4.0), 3Q2A correction factor table, and RAP predictor are publicly available at regenvolume3d.org.

Ethical Approval

Micro-CT data from animal models were obtained under Austrian animal ethics approval (CETU-AI-2024-021). Human clinical MRI datasets were obtained under ethics approvals from contributing clinical centres. No new subject research was conducted.

ISSN: e-ISSN: 3117-6445 / p-ISSN: 3117-6453 Vol: 2025, Issues: 2, 2025

Appendix A

RT3RA Implementation and RegenVolume Specifications

The following provides RT3RA component implementation details and RegenVolume dataset specifications.

M3SN and TAQ Implementation

VNA and 3Q2A Implementation

RAP and RegenVolume Specifications